

# THE APPLICATION OF RUBBER MATERIAL MODELS TO ANALYSE FLEXIBLE ADHESIVE JOINTS

LE Crocker\*, BC Duncan\*, JM Urquhart\*, RG Hughes\* and A Olusanya†

## INTRODUCTION

Finite Element analysis (FEA) is widely used to predict deformations and stress distributions in adhesive joints (1). The ability to predict these and, hence, the failure of the joint using FEA depends on two main factors; the choice of material model and the reliability of the data input into the model. Flexible adhesives exhibit low moduli and large strains to failure in relation to structural adhesives, such as epoxies. In general, they have been used in non-structural applications but, as design philosophies change, flexible adhesives are becoming used in applications where the mechanical performance of the joint is more critical. Elastic-Plastic material models that may be adequate for structural adhesives are unlikely to accurately represent flexible adhesives at, or above, their glass transition temperature ( $T_g$ ).

As part of the DTI sponsored Performance of Adhesive Joints programme, of under-pinning materials measurement research, an approach has been adopted which models the flexible adhesive as having rubber-like properties. Large strain behaviour of rubbers can be modelled using hyperelastic material models available in FEA packages such as ABAQUS (2). This paper describes an initial evaluation of the capability of Elastic, Elastic-Plastic (von Mises), Hyperelastic (Mooney-Rivlin, Ogden) and Hyperfoam models to characterise a range of flexible adhesives.

In the simplest approximation, the mechanical properties data for characterising the adhesives (such as Young's modulus and Poisson's ratio) can be obtained from uniaxial tension tests on bulk specimens. However, data under different states of stress are desirable to model multi-axial stresses in the adhesive joints. Coefficients used to characterise the hyperelastic material properties can be derived from uniaxial tension, plane strain (planar tension) and equibiaxial tension test data.

Strain energy concepts are commonly used to predict rupture of rubbers (3,4). Therefore, a failure criterion based on the strain energy at failure has been investigated. Elastic strain energies to break were obtained from uniaxial tensile tests on bulk samples. Three commercial adhesives 3M DP609 (2-part polyurethane), Evode M70 (1-part polybutadiene) and PPG3289Y5000 (1-part epoxy-butadiene) have been studied. Bulk and lap joint specimens have been tested over a range of temperatures. FE analyses on the lap joint were performed to evaluate the various models through the predicted deformations and elastic strain energies.

## FINITE ELEMENT MODELS

FEA was carried out to predict the behaviour of simple lap joints using the data derived from bulk specimen tests. The material function library in ABAQUS includes several models of elastic behaviour. The following ABAQUS models were selected; Elastic, Elastic-Plastic, Hyperelastic (Mooney-Rivlin and Ogden) and Hyperfoam. These models are described below.

---

\* National Physical Laboratory, Teddington, UK, TW11 OLW

† Now with Loctite, Dublin

The Elastic model, the simplest of the material models investigated, uses the linear relationship between stress and strain. This is normally only valid for small strains. For an isotropic material, the elastic properties are defined by the Young's modulus,  $E$ , and Poisson's ratio,  $\nu$ . The Elastic-Plastic model uses the classical metal plasticity (von Mises) yield surface to define isotropic yielding. This is unlikely to accurately characterise polymeric adhesives. To define the plasticity data in ABAQUS, the true yield stress of the material as a function of true plastic strain is required. Pressure sensitive yield criteria such as the Drucker-Prager, although not investigated in the present work, may provide more realistic yield descriptions. At low strains the material has approximate linear behaviour. At higher stress (and strain) magnitudes the material begins to exhibit nonlinear, irrecoverable behaviour (known as plasticity).

The stress-strain behaviour of rubbers is elastic (i.e. recoverable) but highly nonlinear. This type of material behaviour is known as hyperelasticity. ABAQUS uses strain energy potentials to relate stresses to strains in hyperelastic materials. Two different forms of strain energy potentials available are: a polynomial model (of which the Mooney-Rivlin is a particular case) and the Ogden model.

The Mooney-Rivlin case is obtained from the polynomial form of the hyperelastic model by setting the polynomial parameter,  $N$ , to one, i.e. the first order polynomial. The Mooney-Rivlin model uses only linear functions of the deviatoric strain invariants. The initial shear modulus,  $\mu_0$ , and the bulk modulus,  $K_0$ , when  $N=1$  are:

$$\mu_0 = 2(C_{10} + C_{01}) \quad (1) \quad ; \quad K_0 = 2/D_1 \quad (2)$$

where  $C_{10}$ ,  $C_{01}$  and  $D_1$  are temperature-dependent material parameters. The  $D_1$  parameter allows for the inclusion of compressibility. However, unless volumetric test data are available,  $D_1$  is assumed to be zero. From equation (2) this leads to an infinite bulk modulus, i.e. incompressibility. To define material properties for the Mooney-Rivlin model, the parameters  $C_{10}$ ,  $C_{01}$ ,  $D_1$ , and temperature are entered in the ABAQUS input file.

The Ogden strain energy potential is expressed in terms of the principle stretches. In ABAQUS, the form of the Ogden strain energy potential is:

$$U = \sum_{i=1}^N \frac{2\mu_i}{\alpha_i^2} (\bar{I}_1^{\alpha_i} + \bar{I}_2^{\alpha_i} + \bar{I}_3^{\alpha_i} - 3) + \sum_{i=1}^N \frac{1}{D_i} (J^{el} - 1)^{2i} \quad (3)$$

where  $\bar{I}_i$  are the deviatoric principle stretches.  $N$  is the order of the polynomial,  $\mu_i$ ,  $\alpha_i$ , and  $D_i$  are temperature-dependent material properties. In this work, a third order polynomial form of the Ogden model was used. To define material properties in ABAQUS using this Ogden model, the following parameters are required;  $\mu_i$ ,  $\alpha_i$  and  $D_i$  ( $i = 1, 2, 3$ ) and temperature. The  $D_i$  terms allow for compressibility, as described above. The initial shear modulus is a function of  $\mu_i$ .

In the absence of volumetric test data, both the Mooney-Rivlin and Ogden models assume that the material is incompressible (i.e.  $\nu = 0.5$  and  $D_i = 0$ ). However, for the adhesives studied, Poisson's ratio is less than 0.5 (i.e. the materials are compressible). An ABAQUS model that takes this compressibility into account is the foam hyperelasticity model (known as Hyperfoam).

The Hyperfoam model uses the strain energy function:

$$U = \sum_{i=1}^N \frac{2m_i}{a_i^2} \left[ \hat{I}_1^{a_i} + \hat{I}_2^{a_i} + \hat{I}_3^{a_i} - 3 + \frac{1}{b_i} \left( (J^{el})^{-a_i b_i} - 1 \right) \right] \quad (4)$$

where  $N$  ( $=1, 2, 3$ ) is the polynomial model order,  $\mu_1$ ,  $\alpha_1$ , and  $\beta_1$  are temperature-dependent material parameters;  $\hat{I}_i = (J^{th})^{-1/3} I_i$ ,  $\hat{I}_1 \hat{I}_2 \hat{I}_3 = J^{el}$  and  $\lambda_i$  are the principle stretches.  $J^{el}$  is the elastic volume ratio and  $J^{th}$  is the thermal volume ratio. The coefficient  $\beta_i$  determines the degree of compressibility and is related to Poisson's ratio,  $\nu_i$ . For this work the first order strain energy potential was used, i.e.  $N = 1$ . The parameters  $\mu_1$ ,  $\alpha_1$ ,  $\nu_1$ , and temperature are entered in the ABAQUS input file.

## EXPERIMENTAL

The hyperelastic models rely on fitted coefficients. It is clear that the ability of a model to predict material behaviour depends strongly on the choice of these coefficients. A convenient way of defining a hyperelastic material is to supply ABAQUS with test data. ABAQUS then calculates the constants using a least-squares method. It is preferable to determine material properties data for input into FE models from tests on bulk test specimens rather than joint test specimens. The larger gauge lengths allow scope for more accurate strain determination and there is no need to account for the influence of the adherends. Many adhesives can be cast into bulk sheets, 1 - 2 mm thick, from which test specimens can be cut (5). However, it is important that the bulk material has similar properties to the material in the joint.

For the simplest material models, the input data can be determined from uniaxial tension tests where stress,  $\sigma$ , strain,  $\epsilon$ , and lateral contractions,  $\epsilon_l$ , are measured. Flexible adhesives have large extensions at failure. Thus, non-contacting strain measurement techniques, such as video extensometry, are required. The drawback of such techniques is that the accuracy at low strains may be less than for contacting methods. The Elastic model requires only the Young's modulus,  $E$ , and Poisson's ratio,  $\nu$ . The Elastic-Plastic model, if von Mises yielding is assumed, requires plastic strain-yield stress data. The plastic strain is obtained from subtracting the elastic strain ( $= \sigma/E$ ) from the total strain ( $\epsilon$ ) at each stress. Yield stresses are simply the true stresses (corrected for the contraction of the specimen) at all non-zero plastic strains.

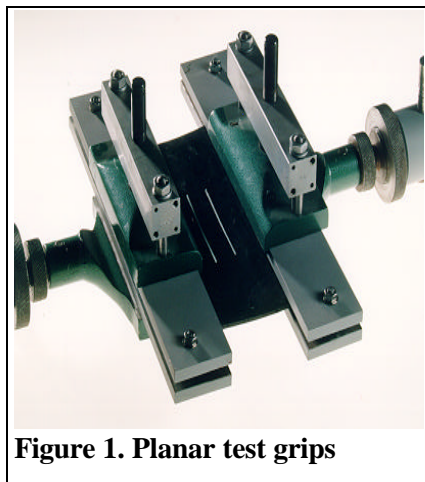


**Figure 1. Planar test grips**

The more complex material models require mechanical properties under additional states of stress. The Hyperelastic (Mooney-Rivlin and Ogden) and Hyperfoam models in ABAQUS use plane strain and equibiaxial stress-strain data in addition to the uniaxial test data. The plane strain (or planar tension) test uses a large aspect ratio specimen (large width, small gauge length) that is securely clamped along the width to restrict the lateral contraction. This type of test is also referred to as a pure shear test. Planar test specimens (80 mm long x 200 mm wide) were tested with a 40 mm gauge length using grips such as those in Figure 1. In an equibiaxial test a symmetrical specimen

is extended to the same degree in two orthogonal directions. This type of test can be carried out using a multi-axial test machine. However, these machines are expensive and rare. Therefore, a scissor-action test frame that fits into a standard test machine was developed (Figure 2). The square specimen (45 mm) is extended at  $\pm 45^\circ$  to the axis of the test machine. The load and extension of the specimen along the axis of the test machine are measured. These are used to resolve the components of stress and strain in the axes of extension. There are a number of assumptions, principally concerning the uniformity of the stress and strain distributions in the specimens, which will be investigated in future work.

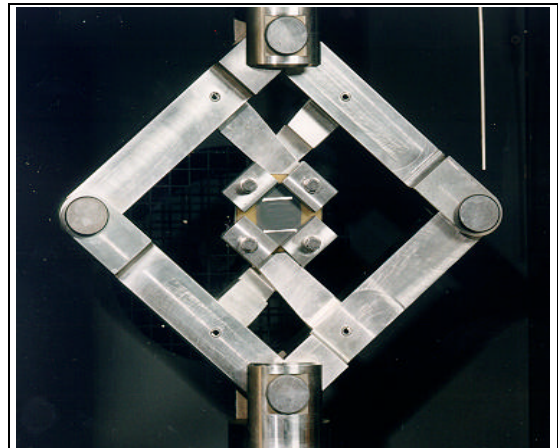


**Figure 2. Equibiaxial test configuration**

Models for rubbers suggest strain energies in the material as failure criteria for predicting material rupture. Failure energies for the bulk test specimens were calculated from the areas under the stress strain curves. The energy dissipated in the adhesive during deformation can be estimated from the area enclosed by the hysteresis loop formed on reversing the test machine at 95% of the expected failure stress of the specimen.

## LAP JOINT TESTING AND MODELLING

Lap joint samples were prepared with zinc coated steel adherends (50 x 25 x 3 mm) giving 12.5 mm bond length and 0.5 mm bond thickness. These adherends were grit blasted and solvent cleaned prior to bonding. The cure schedules used were the same as for the bulk

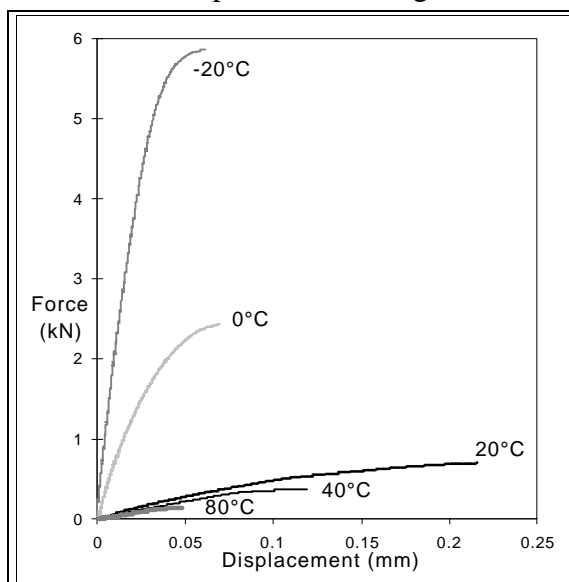


**Figure 3. Force-displacement curves for DP609 lap joints**

specimens. Upon testing, the DP609 lap joints showed increasing stiffness with decreasing temperatures as expected (Figure 3). The lap joints tested at 20°C have the highest extension to failure (when the adhesive is close to its  $T_g$ ). However, these tests show the most scatter. Above 20°C, the extension to failure decreased with increasing temperature. These findings agree qualitatively with tensile test results. The PPGY5000 adhesive is in a rubbery state at all temperatures, and all lap joint force-displacement curves were fairly repeatable. The same is also true for M70 lap joints. The DP609 and PPGY5000 lap joints failed prematurely in an adhesive mode at relatively low extensions (0.1-0.2 mm). The M70 joints tended to fail cohesively at much larger extensions (>0.5 mm).

The lap joint was modelled using a 2-dimensional model. The 2-D continuum plane strain element CPE8RH (2) was used. The mesh was most refined in the adhesive region of the joint. The free end of one adherend was fully constrained. The end of the other adhesive was

constrained only in the y-direction. This end was displaced by a set distance in the x-direction, along the length axis of the specimen. Analyses were run at various temperatures. At each temperature, the lap joint model was subjected to a series of different free-end displacements. These displacements ranged from 0.05 mm to 1 mm. The outputs obtained from each analysis included the force-displacement curve and tables of energy outputs.

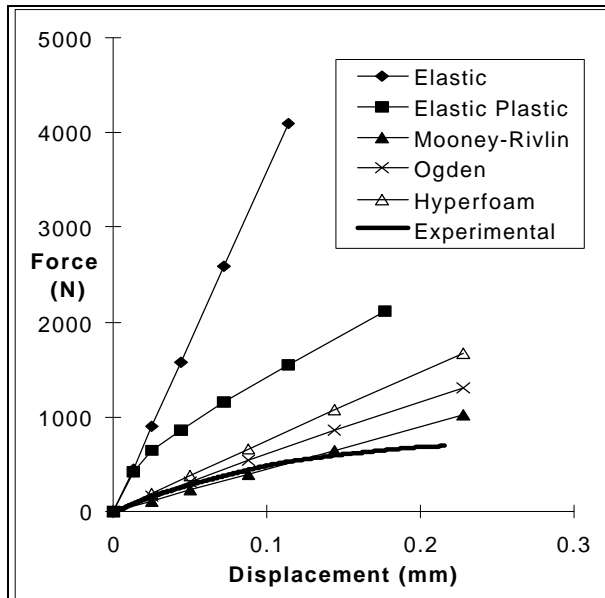


**Figure 4. Comparison of DP609 lap joint FE predictions with experimental results at 20°C**

Initial comparisons between the predicted and measured joint behaviours have shown that above  $T_g$  the hyperelastic models tend to give the best agreements with the lap joint test data. The correlation of the Elastic and Elastic-Plastic model predictions with the experimental data tended to be poor even at low strains. This is unexpected as the Elastic behaviour prediction ought to be reasonably accurate (provided that the material properties of the joints and the bulk specimens are the same).

A typical comparison between the material model predictions and the experimental lap joint data is illustrated in Figure 4. Figure 4 shows DP609 at 20°C (roughly  $T_g$ ). The extension to failure of bulk and lap joint specimens was highest in this region. The

Elastic and the Elastic-Plastic models significantly overestimate the stiffness of the joint. The hyperelastic models agree better with the test data. However, all predictions are much more linear than the lap joint force-displacement curve. The higher degree of curvature in the test data may be due to the onset of peeling in the test which reduces the load bearing area.

One of the aims of the FE analysis is to predict the failure energy of a joint and to compare this to the experimentally measured failure energy in bulk samples. The lap joint ‘failure displacements’ are needed to obtain a value for comparison. For each data set, the failure displacement was taken as the displacement at maximum load for a typical sample. None of these displacements correlated with the displacements used for the FE analyses. The strain energy for the failure displacement was obtained by interpolating between the FE predicted energies at known displacements.

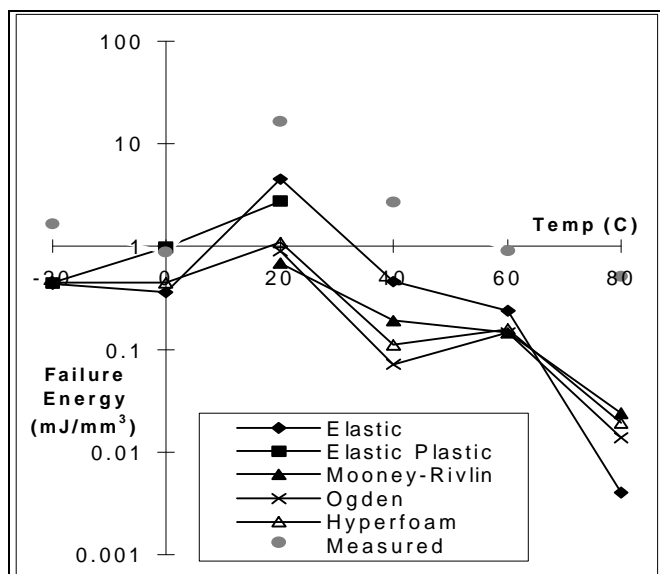


**Figure 5. Comparison of predicted failure energies with experimentally measured failure energies for DP609 adhesive**

For the DP609 adhesive (Figure 5) the failure energies experimentally measured from bulk samples are higher than those

predicted by FEA. All DP609 lap joints failed prematurely at small displacements due to the adhesive peeling away from the adherends. The model predictions and the experimental measurements follow the same trends and show that the failure energy is largest around 20°C. This corresponds to the glass transition temperature of this adhesive. The failure was caused by poor adhesion strength. It is thought that more extensive surface preparation would have changed the failure mode to cohesive. In this case, it is likely that displacements at failure and, hence, failure energies would have been much greater. For the M70 and PPGY5000 adhesives, the FE predicted failure energies were higher than the measured energies. Bulk samples of these adhesives failed prematurely due to the presence of air bubbles.

## **CONCLUSIONS**

Five FE material models that may be used to characterise flexible adhesives have been investigated. Tests to obtain the material properties required to determine the input coefficients have been developed. An initial evaluation of the capability of these models to predict the experimental force-displacement curves obtained from the lap joint specimens has been undertaken. The hyperelastic models give the best agreement with the lap joint tests, although predicted force-displacement curves tended to be much more linear than those measured experimentally. The Elastic model is clearly unsuitable. The Elastic-Plastic model data indicate that the von Mises yield criterion is not appropriate for these materials. There are other yield criteria available in ABAQUS and it is recommended that the validity of these models is explored in future work.

The failure energies obtained from uniaxial tests on bulk samples were compared with those predicted by FEA. For the PPGY5000 and M70 adhesives, the predicted failure energies were higher than the measured failure energies for bulk tensile specimens. For DP609, the predicted failure energies were below those measured experimentally. However, the trends with temperature in the predicted and measured failure energies were similar. Premature failure of bulk specimens through the presence of voids (M70 and PPGY5000) or joints due to inadequate surface preparation (DP609) makes any evaluation of the strain energy failure criterion unreliable. This initial study has indicated that the hyperelastic models show most promise for characterising flexible adhesives but that further work is required on techniques for obtaining input data.

## **ACKNOWLEDGEMENTS**

This work was funded by the DTI under the Materials Metrology Performance of Adhesive Joints Programme.

## **REFERENCES**

1. Charalambides M.N. and Olusanya A., NPL Report CMMT(B)131, April 1997
2. ABAQUS/Standard User's and Theory Manuals, Version 5.8, Hibbit, Karlsson & Sorenson Inc., USA, 1998
3. Grosch K., Harwood J.A.C. and Payne A.R., Nature, 212, 496 (1966)
4. Harwood J.A.C. and Payne A.R., J Appl. Polymer Sci, 12, 889 (1968)
5. Girardi M. and Duncan B., Structural Adhesives in Engineering IV, July 1995, 227